RAPID COMMUNICATION

Synthesis of large FeSe superconductor crystals via ion release/introduction and property characterization*

Dongna Yuan(苑冬娜)[1], Yulong Huang(黄裕龙)[1], Shunli Ni(倪顺利)[1], Huaxue Zhou(周花雪)[1], Yiyuan Mao(毛义元)[1], Wei Hu(胡卫)[1], Jie Yuan(袁洁)[1], Kui Jin(金魁)[1,2], Guangming Zhang(张广铭)[3], Xiaoli Dong(董晓莉)[1,2,†], and Fang Zhou(周放)[1,2,‡]

[1] *Beijing National Laboratory for Condensed Matter Physics, Institute of Physics, Chinese Academy of Science, Beijing* 100190, *China*
[2] *University of Chinese Academy of Sciences, Beijing* 100049, *China*
[3] *State Key Laboratory of Low Dimensional Quantum Physics and Department of Physics, Tsinghua University, Beijing* 100084, *China*

(Received 25 May 2016; revised manuscript received 30 May 2016; published online 9 June 2016)

Large superconducting FeSe crystals of (001) orientation have been prepared via a hydrothermal ion release/introduction route for the first time. The hydrothermally derived FeSe crystals are up to 10 mm×5 mm×0.3 mm in dimension. The pure tetragonal FeSe phase has been confirmed by x-ray diffraction (XRD) and the composition determined by both inductively coupled plasma atomic emission spectroscopy (ICP-AES) and energy dispersive x-ray spectroscopy (EDX). The superconducting transition of the FeSe samples has been characterized by magnetic and transport measurements. The zero-temperature upper critical field H_{c2} is calculated to be 13.2–16.7 T from a two-band model. The normal-state cooperative paramagnetism is found to be predominated by strong spin frustrations below the characteristic temperature T_{sn}, where the Ising spin nematicity has been discerned in the FeSe superconductor crystals as reported elsewhere.

Keywords: FeSe superconductor, hydrothermal growth via ion release/introduction, upper critical field, spin frustrations

PACS: 74.70.Xa, 81.10.–h, 74.25.Op, 75.10.Jm **DOI:** 10.1088/1674-1056/25/7/077404

The tetragonal FeSe superconductor, formed by a stacking of edge-sharing $FeSe_4$-tetrahedra layers, was reported to show the bulk superconducting transition at $T_c \sim 8$ K.[1,2] It is notable that its T_c can be enhanced to 36.7 K under high pressure[3–6] and to ~ 48 K by charge injection.[7] Other more complicated iron selenide superconductors such as $A_yFe_{2-x}Se_2$ and $(Li_{1-x}Fe_x)OHFe_{1-y}Se$ can be viewed as derived from the binary FeSe by intercalating the alkali metal ions A and the spacer layer $(Li_{1-x}Fe_x)OH$ in between the adjacent $FeSe_4$-tetrahedra layers, respectively. The FeSe layers are common to all the iron selenides and serve as the basic superconducting unit. Therefore, the simplest binary FeSe superconductor is thought to be an important prototype for investigating the underlying physics of the superconductivity.

In FeSe, no antiferromagnetic long-range order exists under ambient pressure, but the rotational symmetry breaking in the electronic structure of the iron plane has drawn much attention.[8–11] Recent neutron scattering results[12–14] suggested that the electron pairing for the superconductivity is closely related to the stripe-like $(\pi, 0)$ antiferromagnetic spin fluctuations and a sharp spin resonance was observed in the superconducting state. However, the tetragonal-to-orthorhombic structure transition at $T_s \sim 90$ K has no spin origin, but is driven, as commonly believed, by the orbital ordering with unequal occupancies of the iron $3d_{xz}/3d_{yz}$ orbitals.[15,16] Most recently, this issue has been resolved by our angular-dependent magnetoresistance (AMR) and magnetism measurements. We have clearly observed the rotational symmetry breaking due to the Ising spin nematicity below a characteristic temperature T_{sn}, and found a universal positive linear relationship between T_c and T_{sn} among various superconducting FeSe samples.[17] These important results were mainly obtained on large (001)-orientating FeSe crystal samples prepared by the hydrothermal ion release/introduction. In this paper, we report the crystal growth and the property characterization of the FeSe samples.

Enough big FeSe crystal samples of (001) plane orientation are required for well-defined in-plane (along the iron plane) and out-of-plane (perpendicular to the iron plane) AMR and magnetic measurements. These measurements have turned out to be the key to uncovering the Ising spin-nematic order in bulk FeSe.[17] Although centimetric-large FeSe superconductor crystals were grown by a specially designed flux-free floating-zone technique in our earlier work,[18] the obtained samples displayed the (101) orientation. The commonly used slow-cooling flux growth[19–23] and the very time-consuming vapor transport process[24–26] produced FeSe crys-

*Project supported by the National Natural Science Foundation of China (Grant Nos. 11574370, 11274358, and 11190020), the National Basic Research Program of China (Grant No. 2013CB921700), and the Strategic Priority Research Program (B) of the Chinese Academy of Sciences (Grant No. XDB07020100).

†Corresponding author. E-mail: dong@iphy.ac.cn
‡Corresponding author. E-mail: fzhou@iphy.ac.cn

© 2016 Chinese Physical Society and IOP Publishing Ltd

tals of millimetric sizes. In most cases, the cleaved surfaces of the as-grown crystals were also along the (101) plane, though the (001) orientation was available in some cases, e.g., the vapor transport growth. The high-efficient synthesis of the (001)-orientating big FeSe crystals reported here is inspired by our recent ion/cluster exchange growth of large $(Li_{0.84}Fe_{0.16})OHFe_{0.98}Se$ superconducting crystals.[27] The structure of insulating $K_{0.8}Fe_{1.6}Se_2$ (the 245 phase with $\sqrt{5}\times\sqrt{5}$ ordered iron vacancies) consists of an alternative stacking of the K monolayer and the $Fe_{0.8}Se$ monolayer similar to the target FeSe compound (Fig. 1(a)), so as to be an ideal matrix for the hydrothermal reaction. Moreover, the $K_{0.8}Fe_{1.6}Se_2$ crystals always show a well cleaved (001) plane. After hydrothermal procedures, the interlayer K ions are completely released and the ordered vacant Fe sites $\sim 20\%$ in amount in the $Fe_{0.8}Se$ layers are occupied by the introduced Fe ions. The yielded end FeSe single crystal naturally inherits the original (001) orientation of the matrix. The separation between the neighboring FeSe layers is shrunk by $\sim 22\%$ (from ~ 7.067 Å for $K_{0.8}Fe_{1.6}Se_2$ to ~ 5.525 Å for FeSe). Figure 1 illustrates this hydrothermal K release and Fe introduction process.

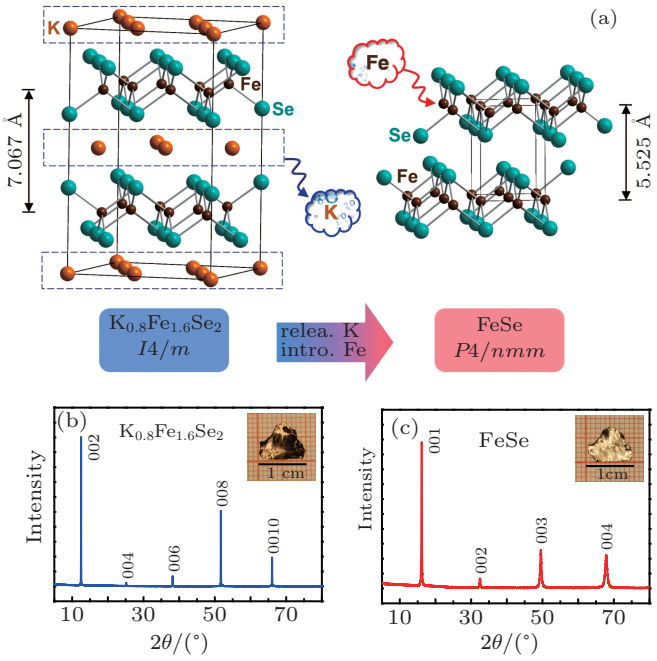


Fig. 1. (color online) (a) Illustration of the hydrothermal K/Fe release/introduction synthesis of the superconducting FeSe crystal from the insulating $K_{0.8}Fe_{1.6}Se_2$ matrix. (b) and (c) XRD patterns of the crystal samples of the matrix $K_{0.8}Fe_{1.6}Se_2$ and the hydrothermally derived FeSe, respectively, all showing single preferred orientations of the (001) planes. The insets are the photographs for the two crystals.

The growth of the $K_{0.8}Fe_{1.6}Se_2$ matrix crystal has been detailed in our recent report (supplemental material of Ref. [27]). The hydrothermal reactions were performed in stainless steel autoclaves of 25 ml capacity with Teflon liners. Large crystal of $K_{0.8}Fe_{1.6}Se_2$, Fe powder (Alfa Aesar, 99.998% purity) of 0.03 mol, and selenourea (Alfa Aesar, 99.97% purity) of 0.06 mol were used as the starting materials. The autoclave loaded with the reagents and 5 ml deionized water was tightly sealed and heated at 120–150 °C for several days depending on the sample conditions to ensure the K-release and Fe-introduction. One difference from our recent ion/cluster exchange growth is that no $LiOHH_2O$ was used as the reagent. The eventually obtained big FeSe crystals, up to 10 mm×5 mm×0.3 mm in dimension, were washed by de-ionized water for several times. The synthesized FeSe crystals are sensitive to atmosphere, so all the data reported for FeSe were measured on the fresh samples. X-ray diffraction on powder and crystal samples of FeSe was carried out at room temperature on a Rigaku Ultima IV (3 KW) diffractometer using Cu K_α radiation, with a 2θ range of 10°–80° and a scanning step of 0.02° (for the powder) or 0.01° (for the crystal). X-ray rocking curve was measured on a double-crystal diffractometer (Rigaku SmartLab, 9 KW) equipped with two Ge (220) monochromators. The chemical composition was determined by both inductively coupled plasma atomic emission spectroscopy (ICP-AES) and energy dispersive x-ray spectroscopy (EDX). The magnetic measurements were conducted on a Quantum Design MPMS-XL1 system of a small remnant field < 4 mOe. The electrical resistivity was measured on a Quantum Design PPMS-9.

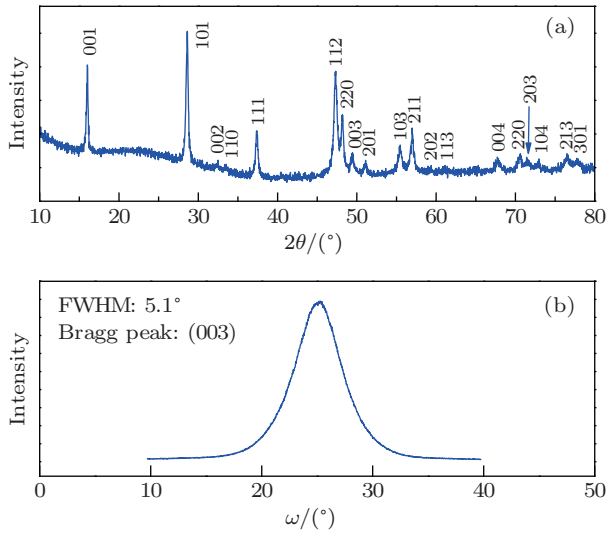


Fig. 2. (color online) (a) Powder XRD pattern for the FeSe crystal ($T_c \sim 7.6$ K). All the diffraction peaks can be well indexed to the previously reported tetragonal unit cell with $a = 3.7725(1)$ Å and $c = 5.5247(2)$ Å. A small quantity (9.28 mg) of the sample was used for the XRD, so the signal-to-noise ratio is not high. (b) Double-crystal XRD rocking curve of the (003) reflection for the FeSe crystal. The surface dimension of the sample is 5 mm×1 mm.

Figure 2(a) shows the powder XRD pattern for a typical FeSe crystal sample. All the diffraction peaks can be well indexed to a previously reported tetragonal structure with the space group of $P4/nmm$, and no impurity phase is detected within the experimental resolution. The lattice constants are

calculated to be $a = 3.7725(1)$ Å and $c = 5.5247(2)$ Å. Figure 2(b) shows the x-ray rocking curve of (003) Bragg reflection. The well symmetrical x-ray rocking curve shows a full-width-at-half maximum (FWHM) of 5.1°, a little smaller than that reported for the FeSe crystals grown by the flux[22] and floating-zone[18] techniques. The chemical composition determined by ICP-AES is Fe : Se= 0.99 : 1 for the typical crystal ($T_c \sim 7.6$ K). No trace of K element in the FeSe sample is detected by EDX, verifying a complete release of K ions during the hydrothermal process. The bulk superconductivity for two hydrothermal FeSe crystal samples ($T_c \sim 6.8$ K and ~ 7.6 K) has been evidenced by the sharp diamagnetic transitions and the 100% diamagnetic shielding signals, as shown in Fig. 3.

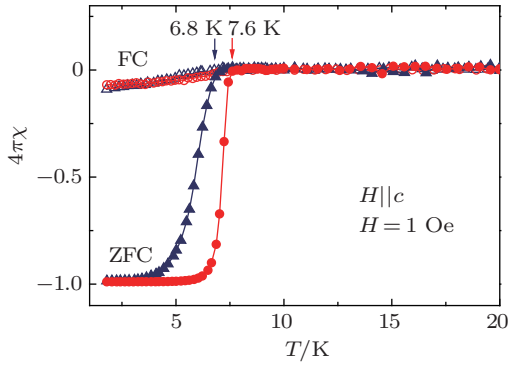


Fig. 3. (color online) Temperature dependence of the static magnetic susceptibility, corrected with the demagnetization factor, near the superconducting transitions for two hydrothermal FeSe crystal samples. The magnetic measurements were performed under $H = 1$ Oe.

The temperature dependence of the normal state resistivity for the hydrothermal samples displays a common metallic behavior in the whole measuring temperature range up to 250 K. Figure 4 displays the in-plane electrical resistance $R_{ab}(T)$ near the superconducting transition under the fields $H||c$-axis. The superconducting transition shifts to lower temperatures with increasing magnetic field up to 9 T. The hollow symbols in the inset of Fig. 4 represent the upper critical fields $H_{c2}(T)$ from the 10%, 50%, and 90% resistance drops. The solid lines in the inset are the fitting results by a two-band s-wave model,[28] yielding the zero-temperature $H_{c2}(T = 0)$ of 13.2 T, 14.9 T, and 16.7 T, respectively.

The neutron scattering results have shown a cooperative paramagnetism in the normal state of FeSe superconductors. The temperature dependence of the static magnetization for the typical FeSe crystal ($T_c \sim 7.6$ K) around ~ 55 K under the in-plane and out-of-plane fields is shown in Fig. 5. Below ~ 55 K, the in-plane magnetization under $H = 0.1$ T exhibits an evident behavior change, leading to the downward curvature (Fig. 5(a)). The key point is that this clear downward feature is strongly dependent on the field magnitude. It fades out when the field is lowered to 0.01 T (Fig. 5(b)). The energy difference between the two magnetic fields is tiny. The potential energy of a single spin in 1 T field is only ~ 0.06 meV from the Bohr magneton ($\mu_B = eh/2m$). Therefore, our observation indicates that the strong quantum spin frustrations predominate in the iron plane. In fact, combined with the two-fold anisotropy in AMR below $T_{sn} \sim 55$ K, the Ising spin nematicity has been discerned on this sample.[17] Theoretically, such Ising spin-nematic order is argued to exist in the strongly frustrated limit of the quantum frustrated spin-1 Heisenberg model. Moreover, the downward feature of the magnetization is weakened when the magnetic field is perpendicular to the iron plane ($H||c$, Fig. 5(c)). Such a behavior signifies the magnetic moments fluctuating mainly in the iron plane, which has been confirmed by recent neutron scattering experiments.[12,14]

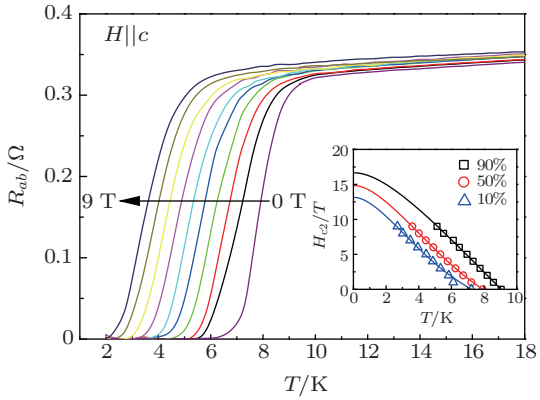


Fig. 4. (color online) The in-plane electrical resistance $R_{ab}(T)$ near the superconducting transition under the magnetic fields up to 9 T. In the inset, the hollow symbols are the upper critical fields $H_{c2}(T)$ from the 10%, 50%, and 90% resistance drops; the solid lines correspond to the $H_{c2}(T)$ fitted by the two-band model, yielding the zero-temperature $H_{c2}(T = 0)$ of 13.2 T, 14.9 T, and 16.7 T, respectively.

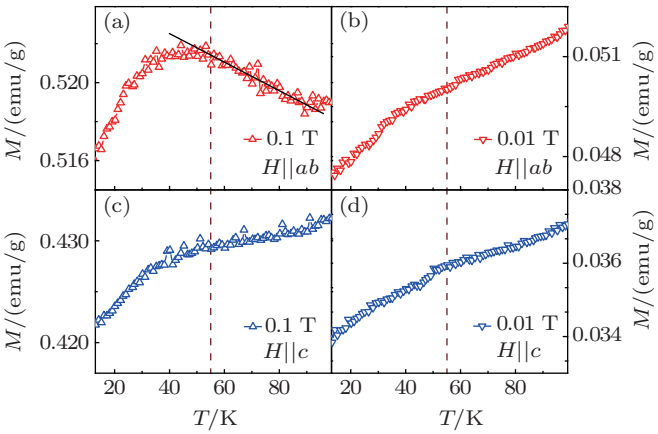


Fig. 5. (color online) Temperature dependence of the static magnetization around ~ 55 K under the in-plane and out-of-plane fields for the typical FeSe crystal ($T_c \sim 7.6$ K). (a) Below ~ 55 K, the magnetization deviates from the linear behavior, leading to the downward curvature. This downward feature strongly depends on both the magnitude and direction of the applied magnetic field, as seen in panels (b) and (c), respectively. (d) The magnetization under the field (0.01 T) perpendicular to the *ab* plane.

To conclude, large and high-quality superconducting FeSe crystals of (001) orientation have been successfully synthesized via the hydrothermal approach by releasing/introducing K/Fe ions out of/into the matrix crystal of

insulating $K_{0.8}Fe_{1.6}Se_2$. This hydrothermal growth is high-efficient (one week) compared to the very time-consuming vapor transport one (months), and is capable of fabricating a series of FeSe samples. Our systematic AMR and magnetic measurements on the FeSe crystal samples have revealed the close relationship between the Ising spin nematicity and the superconductivity in bulk FeSe, which has been reported elsewhere. In addition, this successful growth technique may be applicable in other layer-structured materials, opening up a new route for preparing and exploring functional material crystals desired for both basic research and application.

References

[1] Hsu F C, Luo J Y, Yeh K W, Chen T K, Huang T W, Wu P M, Lee Y C, Huang Y L, Chu Y Y, Yan D C and Wu M K 2008 *Proc. Natl. Acad. Sci. US A* **105** 14262

[2] Mcqueen T M, Huang Q, Ksenofontov V, Felser C, Xu Q, Zandbergen H, Hor Y S, Allred J, Williams A J, Qu D, Checkelsky J, Ong N P and Cava R J 2009 *Phys. Rev. B* **79** 014522

[3] Medvedev S, Mcqueen T M, Troyan I A, Palasyuk T, Eremets M I, Cava R J, Naghavi S, Casper F, Ksenofontov V, Wortmann G and Felser C 2009 *Nat. Mater.* **8** 630

[4] Bendele M, Amato A, Conder K, Elender M, Keller H, Klauss H H, Luetkens H, Pomjakushina E, Raselli A and Khasanov R 2010 *Phys. Rev. Lett.* **104** 087003

[5] Sun J P, Matsuura K, Ye G Z, Mizukami Y, Shimozawa M, Matsubayashi K, Yamashita M, Watashige T, Kasahara S, Matsuda Y, Yan J Q, Sales B C, Uwatoko Y, Cheng J G and Shibauchi T 2015 arXiv1512.06951

[6] Terashima T, Kikugawa N, Kasahara S, Watashige T, Matsuda Y, Shibauchi T and Uji S 2016 arXiv1603.03487

[7] Lei B, Cui J H, Xiang Z J, Shang C, Wang N Z, Ye G J, Luo X G, Wu T, Sun Z and Chen X H 2016 *Phys. Rev. Lett.* **116** 077002

[8] Böhmer A E and Meingast C 2015 arXiv1505.05120

[9] Glasbrenner J K, Mazin I I, Jeschke H O, Hirschfeld P J, Fernandes R M and Valenti R 2015 *Nat. Phys.* **11** 953

[10] Chubukov A V, Fernandes R M and Schmalian J 2015 *Phys. Rev. B* **91** 201105

[11] Chubukov A V, Khodas M and Fernandes R M 2016 arXiv1602.05503

[12] Rahn M C, Ewings R A, Sedlmaier S J, Clarke S J and Boothroyd A T 2015 *Phys. Rev. B* **91** 180501

[13] Wang Q, Shen Y, Pan B, Zhang X, Ikeuchi K, Iida K, Christianson A D, Walker H C, Adroja D T, Abdel-Hafiez M, Chen X, Chareev D A, Vasiliev A N and Zhao J 2015 arXiv1511.02485

[14] Wang Q S, Shen Y, Pan B Y, Hao Y Q, Ma M W, Zhou F, Steffens P, Schmalzl K, Forrest T R, Abdel-Hafiez M, Chen X J, Chareev D A, Vasiliev A N, Bourges P, Sidis Y, Cao H B and Zhao J 2016 *Nat. Mater.* **15** 159

[15] Shimojima T, Suzuki Y, Sonobe T, Nakamura A, Sakano M, Omachi J, Yoshioka K, Kuwata Gonokami M, Ono K, Kumigashira H, Böhmer A E, Hardy F, Wolf T, Meingast C, Löhneysen H v, Ikeda H and Ishizaka K 2014 *Phys. Rev. B* **90** 121111

[16] Baek S H, Efremov D V, Ok J M, Kim J S, Van Den Brink J and Buchner B 2015 *Nat. Mater.* **14** 210

[17] Yuan D N, Yuan J, Huang Y L, Ni S L, Feng Z P, Zhou H X, Mao Y Y, Jin K, Zhang G M, Dong X L, Zhou F and Zhao Z X 2016 arXiv:1605.01507

[18] Ma M W, Yuan D N, Wu Y, Zhou H X, Dong X L and Zhou F 2014 *Supercond. Sci. Technol.* **27** 122001

[19] Zhang S B, Sun Y P, Zhu X D, Zhu X B, Wang B S, Li G, Lei H C, Luo X, Yang Z R, Song W H and Dai J M 2009 *Supercond. Sci. Technol.* **22** 015020

[20] Chareev D, Osadchii E, Kuzmicheva T, Lin J Y, Kuzmichev S, Volkova O and Vasiliev A 2013 *Cryst. Eng. Commun.* **15** 1989

[21] Rao S M, Mok B H, Ling M C, Ke C T, Chen T C, Tsai I M, Lin Y L, Liu H L, Chen C L, Hsu F C, Huang T W, Wu T B and Wu M K 2011 *J. Appl. Phys.* **110** 113919

[22] Ma M W, Yuan D N, Wu Y, Dong X L and Zhou F 2014 *Phys. C* **506** 154

[23] Hu R W, Lei H C, Abeykoon M, Bozin E S, Billinge S J L, Warren J B, Siegrist T and Petrovic C 2011 *Phys. Rev. B* **83** 224502

[24] Koz C, Schmidt M, Borrmann H, Burkhardt U, Rößler S, Carrillo Cabrera W, Schnelle W, Schwarz U and Grin Y 2014 *Z. Anorg. Allg. Chem.* **640** 1600

[25] Patel U, Hua J, Yu S H, Avci S, Xiao Z L, Claus H, Schlueter J, Vlasko-Vlasov V V, Welp U and Kwok W K 2009 *Appl. Phys. Lett.* **94** 082508

[26] Karlsson S, Strobel P, Sulpice A, Marcenat C, Legendre M, Gay F, Pairis S, Leynaud O and Toulemonde P 2015 *Supercond. Sci. Technol.* **28** 105009

[27] Dong X L, Jin K, Yuan D N, Zhou H X, Yuan J, Huang Y L, Hua W, Sun J L, Zheng P, Hu W, Mao Y Y, Ma M W, Zhang G M, Zhou F and Zhao Z X 2015 *Phys. Rev. B* **92** 064515

[28] Gurevich A 2003 *Phys. Rev. B* **67** 184515